Target normal sheath acceleration: theory, comparison with experiments and future perspectives

Target normal sheath acceleration: theory, comparison with experiments and future perspectives

Matteo Passoni[1,2,3,4]**, Luca Bertagna**[1] **and Alessandro Zani**[1]

[1] Dipartimento di Energia, Politecnico di Milano, Via Ponzio 34/3,
20133 Milan, Italy
[2] Istituto di Fisica del Plasma, Consiglio Nazionale delle Ricerche, Milan, Italy
[3] Sezione di Milano INFN, Milan, Italy
E-mail: matteo.passoni@polimi.it

Abstract. Ions can be effectively accelerated during the interaction of an ultra-intense ultra-short laser pulse irradiating a thin solid target via the so-called target normal sheath acceleration (TNSA) mechanism. One of the pivotal questions at this stage of the research is how to predict the properties of the accelerated ions, both from a fundamental point of view and in the light of foreseen applications. In this context, it is desirable to have a simple but reliable description to be used to extrapolate current results to future regimes, which will be made available in the near future, thanks to developments in laser technology. In this paper, the possible approaches for an analytical description of TNSA are discussed, and a theoretical TNSA model is developed. This model is then used to investigate the maximum ion energy as a function of laser parameters. Detailed comparisons with available experimental data and scaling laws are presented. In particular, the relative role played by both the laser pulse energy and irradiance in determining the ion features is investigated.

[4] Author to whom any correspondence should be addressed.

Contents

1. Introduction

The first 10 years of research in the field of ultra-intense laser-induced ion acceleration, started with the pioneering results reported by the Vulcan group [1] and the Nova group [2], transformed this topic into one of the most exciting and active areas of theoretical and experimental physics. The increased capabilities in controlling the various experimental parameters in the complex system formed by the laser pulse and the solid target have led to the achievement of amazing results. In particular, the most recent experiments are performed using laser pulses with improved control of the laser pre-pulse features as well as the temporal and spatial profile, and increasing attention is devoted to detailed control and tailoring of both target properties and interaction conditions. An important consequence is also that, by collecting the experimental results obtained in the various laboratories all over the world, a significant amount of data is now available and potentially useful for a systematic investigation, in the attempt to achieve a satisfactory understanding of the nontrivial underlying physics. Several processes can be responsible for laser ion acceleration, depending on the laser properties and interaction conditions [3, 4]. Most of the present experiments rely on the so-called target normal sheath acceleration (TNSA) mechanism [5]. TNSA allowed the production of very energetic (multi-tens MeV) ion populations. Recently, several other schemes, which should be achieved with proper choices of the laser and/or target properties, have been proposed in order to overcome several drawbacks which actually characterize TNSA, like the low conversion efficiency and the difficulties in producing beams with monochromatic spectrum. Among others, it is worth mentioning the so-called radiation pressure acceleration (RPA) [6]–[8]. Nevertheless, in the next few years TNSA will certainly continue to play a fundamental role, especially because a new generation of laser facilities is becoming available. This will open the way to explore the TNSA regime with a new set of laser parameters so far not possible. All these facts demand a deeper theoretical understanding of TNSA. In particular, an extensive parametric investigation based on a satisfactory theory is definitely required, together with detailed comparisons with the experimental evidence. Besides fundamental interest, these issues are particularly significant also in the light of the envisioned possible applications, for example in the field of inertial fusion via proton-driven fast ignition and in medical applications (production of radioisotopes and hadrontherapy).

     The present paper is devoted to this subject and it is aimed at providing advances in these directions. The main focus will be on one of the most important features of the accelerated

ions, namely the maximum ion energy. In section 2, we start discussing the possible approaches aimed at a theoretical description of TNSA and developing the analytical TNSA theory which will be used in this work. In section 3, the fundamental issue of the dependence of the maximum ion energy on laser parameters, with particular attention to the effective dependence on laser intensity, is addressed, both from a theoretical point of view and through a comparison of the theoretical predictions with available experimental data. Then, a look at the maximum TNSA ion energy corresponding to laser parameters which will be available in the near future follows. Concluding remarks are given in section 4.

2. Theoretical description of the TNSA: a relativistic quasi-static approach

Ions can be accelerated as a consequence of different physical processes, taking place in different regions of the target. A common feature of these mechanisms is that ions are accelerated by intense electric fields, which develop as a consequence of strong charge separations directly or indirectly induced by the laser–matter interaction. At least two qualitatively distinct main sources of charge displacements, possibly acting simultaneously, can be identified. The first is due to the direct action of the laser ponderomotive force on the electrons at the front surface and is the basis of the RPA process [6]–[8]. The second is due to the fact that part of the laser radiation is usually efficiently converted, through various mechanisms, into kinetic energy of a relativistically hot ($T_h \approx$ few MeV) collisionless electron population. These electrons move and recirculate through the solid target, appearing at the surfaces where a cloud of relativistic electrons is formed, extending in vacuum for several Debye lengths, and giving rise to an extremely intense longitudinal electric field, which is responsible for the efficient ion acceleration [1, 2], leading to the TNSA process [5]. In most common conditions, the most effective acceleration mechanism takes place at the rear side of the target, leading to ion acceleration at energies much higher than the laser ponderomotive energy Φ_{pm} (for $I_L = 10^{20}\,W\,cm^{-2}$, $\Phi_{pm} = 6\,MeV$). Recently, the possibility of achieving TNSA also at the front surface has been experimentally demonstrated [9], taking advantage of the use of laser pulses with ultrahigh contrast (UHC), which do not appreciably perturb the surface.

In the following, an analytical description of the TNSA mechanism is developed, and subsequently used to investigate critical issues of this acceleration process.

2.1. Theoretical framework and basic assumptions

By looking in more detail at the physical phenomena which lead to the final ion acceleration in TNSA, we can identify the existence of at least two qualitatively different electron populations in the system. The first is the hot electron component, directly created by the laser pulse in the plasma plume at the front surface of the target. These electrons form a beam propagating normally to the target surface, with typical divergence between 5° and 15°. The density of this electron population is of the order of the critical density (10^{20}–$10^{21}\,cm^{-3}$) and its temperature is of the order of the laser ponderomotive potential. The free motion of this hot electron beam through the target requires the presence of a return current that locally compensates the flow of the hot (and fast) electron component [10]. The return current in metallic targets is provided by a second electron species, the conduction electrons, which are put in motion by the electric field generated by the fast electrons. In insulators, the background free electron population is created by field and thermal ionization. Since the density of the background electron population

in both cases is of the order of the solid density, that is, much bigger than the fast electron density, the required velocity for current neutralization is small and their temperature is much lower than that of the hot electrons. However, this cold and dense electron population can be ohmically heated [10]. To conclude, the electric field generated in TNSA at the vacuum–solid interfaces depends on both the physical parameters of these two electron populations, which are related to the laser–solid interaction on the front surface, and on the transport of the hot component through the target and the heating of the background electrons. The acceleration is most effective on light ions (and specifically protons), which are usually present on target surfaces in the form of contaminants like hydrocarbons and water, or can be present among the constituents of the solid target (e.g. as in plastic targets). The heaviest ion population of the target (possibly constituted of several ion species) provides a positive charge, which offers much more inertia and makes the charge separation responsible for the huge accelerating field. Part of this heavy population can also be effectively accelerated, on a longer time scale, if the protons are not enough to acquire most of the energy contained in the electric field, or if protons are removed before the arrival of the laser pulse, for example, heating the target and/or using other cleaning techniques.

Based on the above discussion, the physics of the TNSA can be theoretically modeled under the following assumptions (which will be further discussed in section 2.3), leading to the formulation of a relatively simple system of equations, which can be investigated analytically and/or numerically. Firstly, let us restrict our analysis to a one-dimensional (1D) geometry. The electron population can be described as a two-temperature distribution, $n_e = n_h + n_c$, where the subscripts 'c' and 'h' refer to the cold and hot electron components, respectively. In addition, we consider the existence of two different ion species, a light (L) and a heavy (H) population: in this way, it is possible to model the most frequent situation in TNSA, namely, the acceleration of light species present on the surfaces of a solid target made of heavy ions. Equations defining the 1D model for the ion acceleration process following from the above assumptions are then the Poisson equation for the self-consistent electrostatic potential $\phi(x, t)$ that takes the form

$$\frac{\partial^2 \phi}{\partial x^2} = 4\pi e(n_e - Z_L n_L - Z_H n_H), \tag{1}$$

and the equations governing the electron and ion dynamics. Generally speaking, they can be described either kinetically (1D Vlasov equation) or with a fluid description, and the resulting system of equations can be investigated numerically (see for example [11]–[16]). Alternatively, the equations can be treated analytically introducing different approximations; their limits of applicability establish the physical regimes where the corresponding solutions hold.

In the sub-picosecond regime, in order to give a suitable description of the process, the inertia of ions is important and the assumption of quasi-neutrality cannot be invoked. A completely different set of approximations can be used in order to analytically investigate the effect of the strong charge separation which can develop, thus describing a physical regime closer to what should produce the most energetic ions. The heavy ions are assumed immobile on the time scale of interest, while the light ions are considered sufficiently few to neglect their effect on the evolution of the electrostatic potential, which in this limit is given by

$$\frac{\partial^2 \phi}{\partial x^2} = 4\pi e[n_e - Z_H n_{0H} H(-x)], \tag{2}$$

where H is the Heaviside function. In order to close the system, the electron density must be properly related to the self-consistent potential ϕ. The effects of the cold electron population

IOP Institute of Physics Φ DEUTSCHE PHYSIKALISCHE GESELLSCHAFT

with a finite thermal energy have been investigated in several publications. For the sake of simplicity, in the following, we will consider $n_c = n_{0c} = \text{constant}$. As far as the high-energy part of the accelerated ion spectrum is concerned, this is a reasonable approximation. Hot electrons are commonly described as having thermal equilibrium in the self-consistent potential, via the Boltzmann relation, $n_e(x) = n_{e0} \exp(e\phi/T)$ [10, 11, 17, 18]. Actually, this apparently reasonable choice poses several difficulties to the analysis, because the self-consistent electrostatic potential diverges at large distance from the target (mathematically, $\phi \to -\infty$ as $x \to +\infty$), which introduces the need for defining artificially a finite acceleration time and/or limited region over which the acceleration is effective in order to avoid divergent maximum ion energy [19]. As a consequence, the fitted acceleration times, often assumed equal or directly related to the laser pulse duration τ_L, usually do not correspond to the physical times over which ion acceleration takes place when $\tau_L < 100 \, \text{fs}$, which has become a quite usual condition in many experimental facilities. It is worth noting that this has nothing to do with the dimensionality of the problem and it is not a pathological consequence of the 1D approximation. On the contrary, it is related to the fact that in a single-charged population in a semi-infinite space, the Boltzmann relation implies particles with infinite kinetic energy, which is not physically meaningful, both because the laser–solid interaction produces electrons with a maximum kinetic energy and/or also because the most energetic electrons overcome the self-consistent potential barrier and are lost by the system [20, 21], as also recently experimentally established [22, 23]. We then describe the hot electrons kinetically, assuming that they follow a 1D, single temperature Maxwell–Jüttner relativistic electron distribution function (edf) in the self-consistent electrostatic potential $\phi(x)$ [24],

$$f_e(x, p) = \frac{\tilde{n}}{2mcK_1(\zeta)} \exp\left(-\frac{W + mc^2}{T}\right), \tag{3}$$

where $W = mc^2(\gamma - 1) - e\phi$, T is the hot electron temperature, $K_1(\zeta)$ the MacDonald function of first order and argument $\zeta = mc^2/T$, where m is the rest electron mass, e the modulus of the electron charge, c the speed of light, $\gamma = (1 + p^2/m^2c^2)^{1/2}$, and the edf has been normalized to the density $\tilde{n}$ by integrating over $-\infty < p < +\infty$. The negatively charged source in the Poisson equation is now given by the bound electron charge density

$$n_b(x) = \int_{W<0} f_e(x, p) \, dp, \tag{4}$$

where the integration extends over the negative energies only. Let us introduce the following dimensionless variables: $\xi = x/\lambda_D$, $\varphi = e\phi/T$, where $\lambda_D^2 = mc^2 K_1/(4\pi \tilde{n} e^2)$. Using equations (2), (3) and (4), the resulting equation for the self-consistent potential is

$$\frac{d^2\varphi}{d\xi^2} = e^\varphi \int_0^{\beta(\varphi)} e^{-\sqrt{p^2+\zeta^2}} \, dp - \frac{(Z_H n_{0H} - n_{0c})}{\tilde{n}} \zeta K_1(\zeta) H(-\xi), \tag{5}$$

where $\beta(\varphi) = \sqrt{(\varphi + \zeta)^2 - \zeta^2}$.

Approximated versions of this equation have been considered in the literature, in the non-relativistic [20] and ultra-relativistic [21] limits, respectively. We will now investigate analytically the exact problem formulated by equation (5).

2.2. Analytical developments

Let us first consider the solution outside the target, namely in the region $\xi > 0$. The Poisson equation can be integrated once and we obtain $\varphi' \equiv \mathrm{d}\varphi/\mathrm{d}\xi$,

$$\frac{\mathrm{d}\varphi}{\mathrm{d}\xi} = -\sqrt{2}\left[\mathrm{e}^{\varphi} I(\varphi) - \mathrm{e}^{-\zeta}\beta\right]^{1/2}, \tag{6}$$

where $I(\varphi) = \int_0^{\beta(\varphi)} \mathrm{e}^{-\sqrt{\zeta^2+p^2}}\mathrm{d}p$ and the constant has been determined by imposing that a $\tilde{\xi}$ exists where $\varphi(\tilde{\xi}) = \varphi'(\tilde{\xi}) = \varphi''(\tilde{\xi}) = 0$.

From this equation an implicit exact solution for the electrostatic potential in vacuum follows:

$$\int_{\varphi_0}^{\varphi(\xi)} \frac{\mathrm{d}\varphi'}{\left(\mathrm{e}^{\varphi'} I(\varphi') - \mathrm{e}^{-\zeta}\beta\right)^{1/2}} = -\sqrt{2}\xi, \tag{7}$$

where $\varphi_0 = \varphi(0)$. This solution can be used in order to determine approximate expressions for φ, in the limits of small and large amplitudes, respectively. It is not difficult to show that

$$\varphi(\xi) = \left[\varphi_0^{1/4} - \frac{\sqrt{2}\sqrt[4]{2\zeta}}{4}\mathrm{e}^{-\zeta/2}\xi\right]^4, \quad \text{for} \quad |\varphi(\xi)| \ll 1,$$

$$\varphi(\xi) = \varphi_0 - 2\ln\left[1 + \frac{\sqrt{C}\xi}{\sqrt{2}}\exp\left(\frac{\varphi_0}{2}\right)\right], \quad \text{for} \quad |\varphi(\xi)| \gg 1, \tag{8}$$

where $C = \int_0^{+\infty} \mathrm{e}^{-\sqrt{\zeta^2+p^2}}\mathrm{d}p$. In the limit $\zeta \ll 1$, equation (8) reduces to the non-relativistic expression [20].

The implicit solution of equation (7) depends on φ_0, which can, in principle, be determined by solving the Poisson equation in the target, for $\xi < 0$,

$$\frac{\mathrm{d}^2\varphi}{\mathrm{d}\xi^2} = \mathrm{e}^{\varphi} I(\varphi) - B, \tag{9}$$

where $B = [(Z_H n_{0H} - n_{0c})/\tilde{n}]\zeta K_1(\zeta)$, and imposing the continuity of φ and of φ' at $\xi = 0$. We assume that, far from $\xi = 0$ inside the target, the plasma becomes locally quasi-neutral, so that

$$B = \mathrm{e}^{\varphi^*} I(\varphi^*),$$

where $\varphi^* = \varphi(\xi = -\xi_d \equiv -d/\lambda_D)$, d being of the same order as the target thickness. By integrating once equation (9), we obtain

$$\frac{\mathrm{d}\varphi}{\mathrm{d}\xi} = -\sqrt{2}\left[\mathrm{e}^{\varphi} I(\varphi) - \mathrm{e}^{-\zeta}\beta - B\varphi - \mathrm{e}^{\varphi^*} I(\varphi^*) - \mathrm{e}^{-\zeta}\beta^* - B\varphi^*\right]^{1/2}, \tag{10}$$

where $\beta^* = \beta(\varphi^*)$ and $\varphi' = 0$ at $\xi = -\xi_d$. By imposing the continuity of the electric field at $\xi = 0$, we can obtain a relation between φ_0 and φ^*:

$$\varphi_0 = \frac{\mathrm{e}^{\varphi^*} I(\varphi^*)(\varphi^* - 1) + \mathrm{e}^{-\zeta}\beta^*}{\mathrm{e}^{\varphi^*} I(\varphi^*)}. \tag{11}$$

We observe that if $T \rightarrow \infty$, $\zeta \rightarrow 0$; it follows that $\beta^* \rightarrow \varphi^*$, $I(\varphi^*) \rightarrow 1 - \mathrm{e}^{-\varphi^*}$ and consequently equation (11) reduces to

$$\varphi_0 = \frac{\mathrm{e}^{\varphi^*}(\varphi^* - 1) + 1}{\mathrm{e}^{\varphi^*} - 1}, \tag{12}$$

which is equal to equation (8) of [21].

The electrostatic potential is fully determined from equations (7) and (11) once φ^* is given. The quantity φ^* represents the normalized maximum kinetic electron energy of the laser produced trapped electrons $\epsilon_{e,\max} = K_{e,\max}/T$. It depends on the physics of the laser–solid coupling. It can be related to experimental data, or taken from suitable numerical simulations, or determined on physical grounds. Here, we will present results in which use is made of the scaling law $\varphi^* \approx 4.8 + 0.8 \ln[E_{\mathrm{L}}(J)]$ proposed in [21] and suitable to investigate TNSA in most common experimental conditions, in particular, those in which targets with thickness in the multi-μm range are used. We will also show that when the hot electron properties are available from computer simulations, even in regimes of interaction that are significantly different (like for example those resulting from the use of targets with sub-μm thickness and pulses with UHC [9]), the present model succeeds in providing correct predictions of fast ion properties.

If a test ion of charge Z is placed at rest at $\xi = 0$, it is accelerated up to a maximum kinetic energy $\varepsilon_{i,\max} = Z\varphi_0(\varphi^*)T$. If we consider a distribution of light ions, forming a thin layer placed in $0 \leqslant \xi \leqslant \delta\xi$, with $\delta\xi \ll \xi_d$ with a given volume density $n_\xi(\xi)$, the resulting final energy spectrum can be easily calculated imposing the conservation of the particle number in phase space. In order to evaluate the maximum ion energy and the energy spectrum, the hot electron temperature must be known. Here, we assume this quantity to be given by the ponderomotive scaling [25]

$$T = mc^2 \left(\sqrt{1 + (I_{\mathrm{L}}\lambda^2 [\mathrm{W\,cm^{-2}\,\mu m^2}]/1.38 \times 10^{18})} - 1 \right), \tag{13}$$

which satisfactorily describes the dependence of T on the laser irradiance $I_{\mathrm{L}}\lambda^2$ in the relativistic regime ($I_{\mathrm{L}}\lambda^2 > 10^{18}\,\mathrm{W\,cm^{-2}\,\mu m^2}$), where one of the most significative absorption mechanisms is the *relativistic $J \times B$ heating* (see [26] for more details). To summarize, with the aid of equations (11) (or (12) when appropriate) and (13), together with a suitable estimate of φ^* the problem of determining the maximum ion energy obtained in a given experimental condition via TNSA is reduced to the use of a few, relatively simple, relations mainly involving the laser parameters. In the general case, the integrals contained in equations (7) and (11) can be very easily performed either with any quadrature method or with the direct use of standard mathematical software. Besides the maximum ion energy, other interesting quantities, like the high-energy part of the ion energy spectrum and the extension of the hot electron cloud (or, equivalently, the extension of the accelerating field) can be obtained for comparison with experimental data. In this context, we note that the target properties, which can influence and modify the features of the laser–solid interaction [9], are here indirectly contained in the estimate of φ^*.

In section 3, this theory will be exploited in order to (i) investigate the parametric dependence of the maximum ion energy on the laser parameters, (ii) compare the results of this model with existing experimental data and (iii) provide predictions on TNSA for laser parameters which are likely to become available in the near future.

2.3. Limits of applicability of the theory

The model described above is definitely stationary. In other words, the electron cloud is assumed neither to be affected by the ions flowing through it nor to evolve during the acceleration process. The first condition requires that the number of the ions which are accelerated be much smaller than that of the hot electrons, $N_i \ll N_e$, and that the characteristic time scale of the heavy ion expansion is longer than the light ion acceleration time. As far as the electron dynamics is concerned, it is assumed that both spatial distribution and temperature do not evolve during the ion acceleration process, although it could be expected that the energy of the hot electrons will decay in time due to their expansion, and to collisional and radiative losses. These issues do not seem to represent a major problem in the determination of the maximum ion energy since the acceleration of those ions, which will be the most energetic, takes place on a time over which the temperature and the entire distribution do not vary appreciably [13]. Nevertheless, a better characterization of the ion acceleration process would incorporate the effects coming from a multi-temperature electron distribution [19], and the temporal evolution of the electron temperature, which could compete with the effect of a finite acceleration length in the determination of the maximum energy gain. Electron cooling has been considered in a few recent papers [13, 14].

In order to consider the ion motion during the acceleration process as 1D, the electron cloud should be spatially uniform in the plane normal to the ion motion. Furthermore, the ion acceleration is expected to be planar if the transverse extension of the ion-enriched layer (the portion of the surface where light ions to be accelerated are concentrated) is smaller than that of the electron cloud.

Finally, the resulting ion energy spectrum will inevitably be affected by several spurious mechanisms, which are expected to broaden the ion energy spectra.

3. Discussion

We start our discussion checking the capabilities of the theory described in section 2 in predicting the maximum ion energy in a TNSA experiment. In order to ascertain this important point, we consider a large number of experimental maximum proton energies that have been reported in the literature in the last 10 years [1, 2, 9, 18], [27]–[38]. In figure 1, the theoretical curves at constant maximum proton energy, $\varepsilon_{i,\max}$, in the plane $(I_L\lambda^2; E_L)$ are shown from 1 MeV up to 50 MeV. Ranges of pulse energy ($10^{-2} < E_L < 10^3$ J) and irradiance ($10^{18} < I_L\lambda^2 < 10^{21}$ W cm^{-2} μm^2) most relevant to present experimental conditions are considered. Experimental maximum proton energies are superimposed (red dots); it is interesting to observe that we are here investigating corresponding experimental laser parameters which can differ by orders of magnitudes ($0.1 < E_L < 500$ J, $40 < \tau_L < 1000$ fs and $10^{18} < I_L\lambda^2 < 3 \times 10^{20}$ W cm^{-2} μm^2). The agreement with the theoretical predictions is satisfactory in all these cases (the relative error is maintained within 10–20%). This fact strongly supports the general theoretical framework which is the basis of the present analytical approach.

The effective dependence of the maximum ion energy on the laser irradiance in TNSA experiments represents one of the most interesting and challenging issues. The present feeling on this problem in the community is well represented by the discussions which can be found in recent papers, like for example those by Borghesi *et al* [39, 40]. There, based on a collection of a large number of experimental data, it is reported that different, non-obvious scalings of the
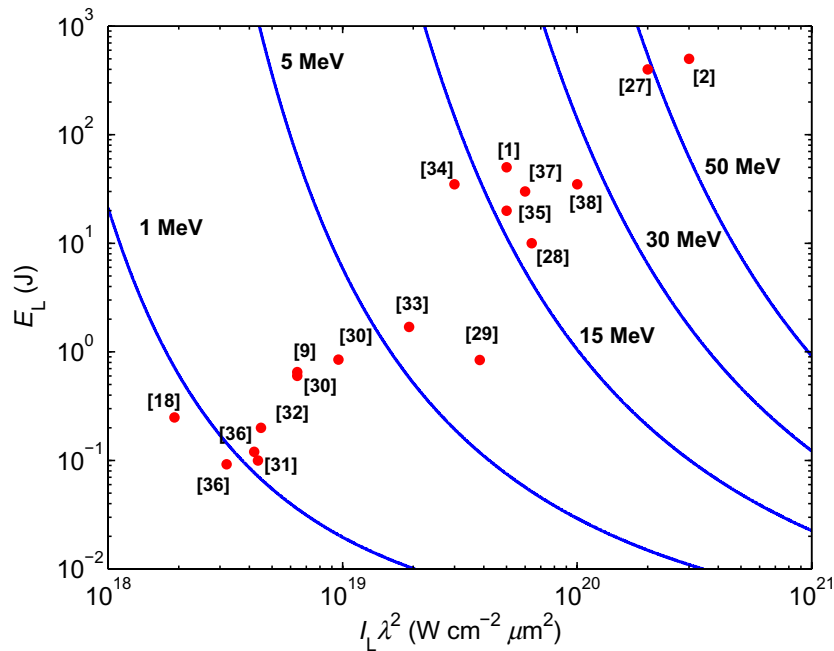
Figure 1. The curves at constant $\varepsilon_{i,\max}$ (in MeV) are plotted in the $(I_L\lambda^2; E_L)$ plane, in units (W cm^{-2} μm^2; J). Ranges relevant for present facilities are considered. A collection of experimental maximum proton energies is superimposed (red dots). Details about the experimental conditions are contained in the corresponding references.
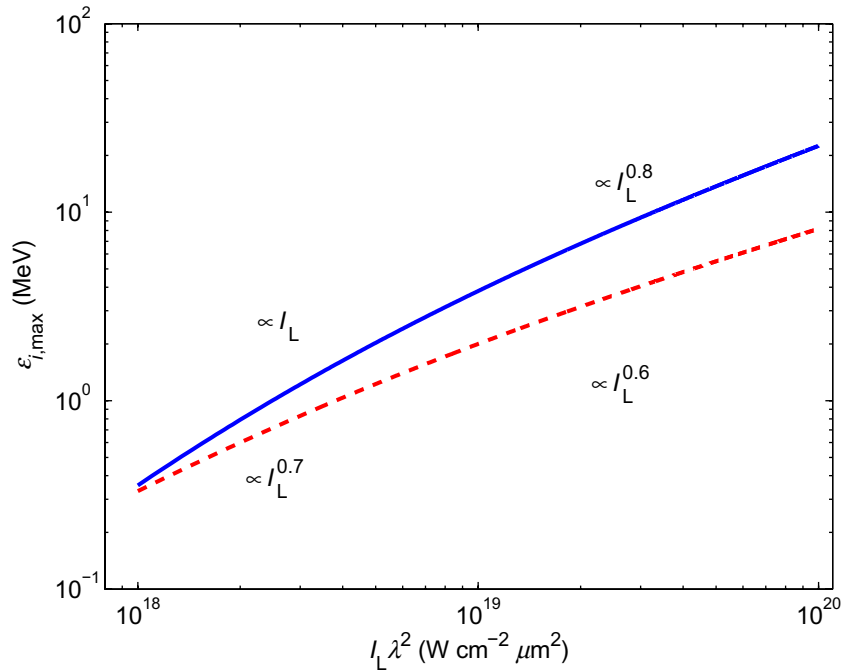
maximum proton energy with the laser irradiance seem to emerge. In particular, an effective almost linear relation is evidenced as characterizing a significant number of results, achieved in various laser facilities. A further, very interesting point is that it has been clearly shown that different maximum ion energies have been produced so far using pulses with the same laser irradiance but with different pulse energy. At present, no satisfactory explanations for these facts have been provided and the underlying physics does not clearly emerge. We used our TNSA theory to investigate this intriguing issue. In figure 2, the maximum proton energy from laser-irradiated targets, for a number of experiments performed on different laser systems, is shown as a function of the pulse irradiance. The experimental values are indicated with blue squares. Also, the fitted effective dependence of the experimental proton energies on the irradiance is plotted (dashed green curve). Actually, the scaling is almost quasi-linear for these data, which refer to pulses with quite different properties: in particular, pulse durations and energies ranging from 40 fs to 1 ps and from 0.1 to 50 J are present, respectively. The corresponding theoretical expectations are indicated with red circles. It can be seen that the observed dependence can be nicely reproduced. We can then interpret the physical situation as the result of the combined, convoluted dependence of the maximum proton energy on the pulse intensity and pulse energy. The point labeled by Ceccotti *et al* [9] deserves a further comment. It does not belong to the described experimental fitting law (actually, it has not been considered in determining it). In that experiment, ultrathin targets in the sub-μm range combined with moderate irradiance, UHC pulses are used. In such systems, a significant enhancement in the maximum ion energy is observed, compared to what can be obtained with the same pulses
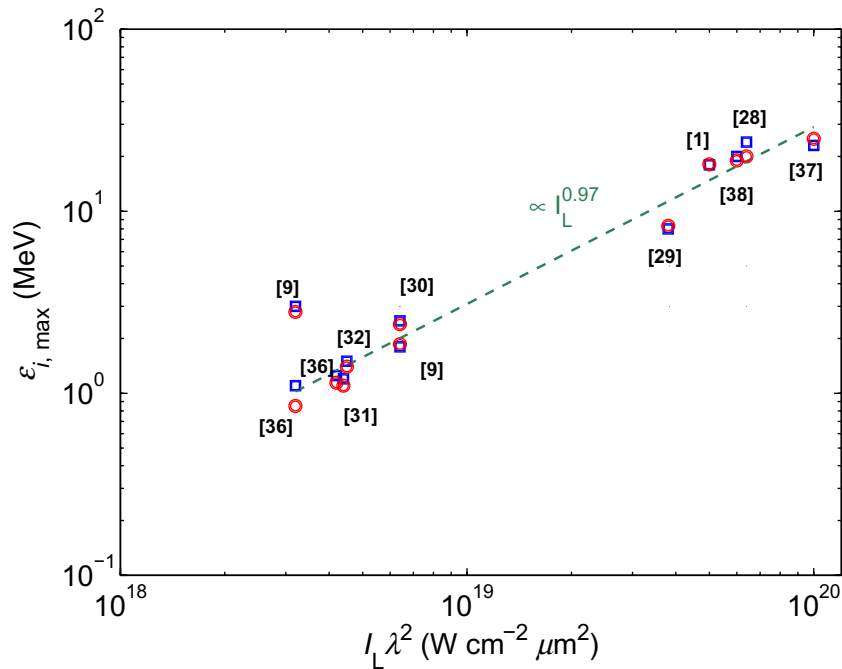
Figure 2. Maximum proton energy from laser-irradiated targets for experiments on different laser systems as a function of the laser pulse irradiance. Experimental values are shown by blue squares, the corresponding theoretical expectations by red circles. Also, the fitted effective dependence of the experimental proton energies on the irradiance is plotted (dashed green curve).

without UHC. Numerical simulations show an increase of the maximum and mean hot electron energy produced in conditions of UHC pulses impinging on ultrathin targets. To estimate the maximum proton energy in this case, we used these numerical results directly to describe the electron properties in equations (11) and (13), and a satisfactory agreement with particle-in-cell (PIC) and experimental values emerges (see also [21] for further details).

In order to draw clear conclusions about both the different possible scaling laws in TNSA and the corresponding underlying mechanisms, dedicated experimental parametric investigations using exactly the same controlled conditions would be greatly valuable. In this connection, it has to be realized that, when results coming from different experiments and performed on different laser facilities are compared, the main quantities that characterize the laser pulse, namely its maximum energy E_L, minimum duration τ_L, focal spot f_L, irradiance $I_L \lambda^2$ and contrast can be very different from each other and, moreover, are not independent parameters. In a given experimental parametric investigation, usually only up to two of these quantities can remain fixed, the others changing simultaneously and accordingly. As a consequence, it is usually quite difficult to extract from a set of experimental data the parametric dependence of the maximum ion energy on a particular laser quantity. On the theoretical side, we can easily simulate such conditions. For the sake of simplicity, we assume that E_L is uniformly contained in the spot f_L, in a temporally rectangular-shaped pulse, so that $I_L = 4E_L/(\tau_L \pi f_L^2)$. As an example, in figure 3, the maximum proton energy $\varepsilon_{i,\max}$ is evaluated as a function of the irradiance $I_L \lambda^2$. Two possible configurations are considered. In the first case (blue, solid

Figure 3. Maximum proton energy $\varepsilon_{i,\max}$ as a function of the pulse irradiance $I_L\lambda^2$, in the interval $10^{18} \leqslant I_L\lambda^2 \leqslant 10^{20}$ (W cm^{-2} μm^2). The laser parameters considered are as follows: blue solid curve: $\tau_L = 25$ fs, $f_L = 20\,\mu$m, $\lambda = 0.8\,\mu$m and the corresponding pulse energy interval is $0.1 \leqslant E_L \leqslant 12$ J; red dashed curve: $E_L = 0.1$ J, $\lambda = 0.8\,\mu$m. The effective power-law fitting is indicated for each irradiance decade.

curve), both the pulse duration and the focal spot are kept fixed, $\tau_L = 25$ fs and $f_L = 20\,\mu$m, respectively; in these conditions, the variation in irradiance is due to a corresponding change in the pulse energy E_L. As a consequence, each simulated pulse corresponds to a specific and different combination of pulse energy E_L and intensity I_L. In the second case, the pulse energy is kept fixed, $E_L = 0.1$ J, the variation in irradiance here being due to a corresponding change in the pulse duration and/or focal spot. This analysis reveals that, if the change in laser intensity is obtained with a corresponding variation in laser energy, the maximum ion energy is characterized by a power-law scaling with I_L which changes with increasing I_L. The power-law is almost quasi-linear in the range $10^{18} \leqslant I_L\lambda^2 \leqslant 10^{20}$ (W cm^{-2} μm^2), in agreement with experimental observations [41]. On the other hand, the dependence becomes almost a square-root law when the change in laser intensity is obtained with a corresponding variation in duration and/or focal spot. Detailed and more extensive theoretical parametric investigations are reported elsewhere [42, 43].

We conclude our discussion extrapolating the predictions of the maximum proton energy in TNSA to future laser parameters, with special focus on ranges which are relevant for most of the latest laboratory facilities. In particular, we consider pulse irradiance $I_L\lambda^2$ and pulse energy in the ranges $10^{20} \leqslant I_L\lambda^2 \leqslant 10^{22}$ W cm^{-2} μm^2 and $1 \leqslant E_L \leqslant 100$ J, respectively. In figure 4, the curves at constant $\varepsilon_{i,\max}$ (in MeV) are plotted in the $(I_L\lambda^2; E_L)$ plane, in units (W cm^{-2} μm^2; J). From these scalings we can predict, as an example, that 100 MeV protons should be obtained
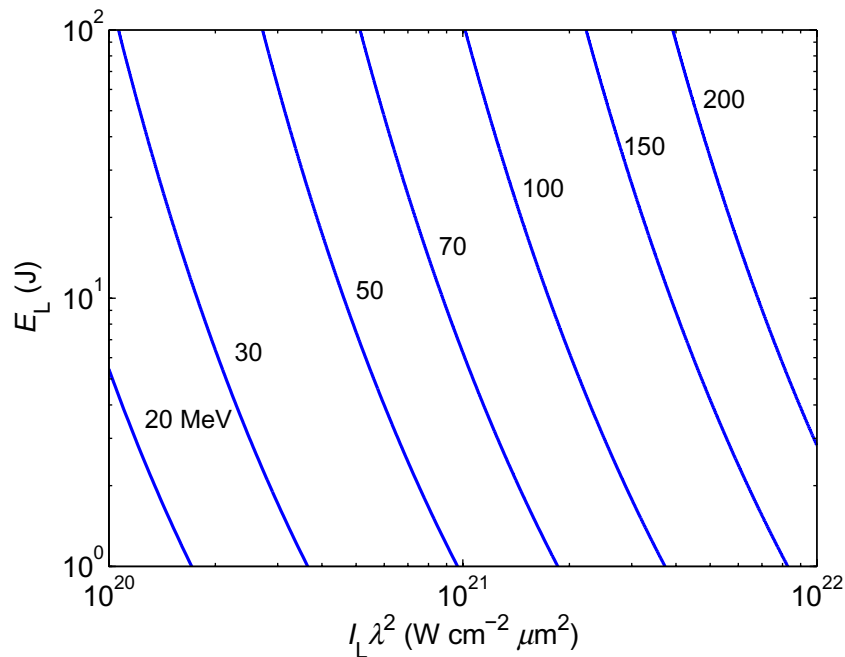
Figure 4. The curves at constant $\varepsilon_{i,\max}$ (in MeV) are plotted in the $(I_L \lambda^2; E_L)$ plane, in units (W cm^{-2} μm^2; J). Ranges relevant for future laser facilities are considered.

with TNSA using laser pulses with $E_L \approx 5.5$ J and $I_L \lambda^2 \approx 2 \times 10^{21}$ (W cm^{-2} μm^2). It is worth noting that at these intensity values the relative importance and the role played by other possibly competitive acceleration mechanisms, such as RPA [44], must be properly taken into account in order to gain a full understanding of the underlying physics.

4. Conclusions

Ion acceleration from solid targets irradiated by high-intensity pulses is an extraordinarily active area of research, currently attracting a surprising amount of experimental and theoretical attention worldwide. Besides fundamental interest, laser-driven ion beams have the potential to be employed in a number of innovative applications in various scientific and technological fields. Simple theoretical modeling of the underlying physics, potentially useful to provide reliable scaling laws and predict the features of the ion beams, which may be produced in the near future with forthcoming laser facilities, represents a major challenge, due to the high complexity of the system. In this work, an analytical description of the TNSA mechanism is developed and used to investigate the properties of accelerated ions as a function of laser and parameters, with the aim to obtain reliable scaling laws. A validation of this model, attained through an extensive comparison with available experimental data, is presented. The resulting scaling laws are also used to predict the maximum energy of the ion beams, which may be produced via TNSA at the extremely high laser intensities which will be made available thanks to the development in laser technology in the next decade.

IOP Institute of Physics ⓓ DEUTSCHE PHYSIKALISCHE GESELLSCHAFT

Acknowledgments

References

[1] Clark E L *et al* 2000 Measurement of energetic proton transport through magnetized plasma from intense laser interactions with solids *Phys. Rev. Lett.* **84** 670

[2] Snavely R A *et al* 2000 Intense high-energy proton beams from petawatt-laser irradiation of solids *Phys. Rev. Lett.* **85** 2945

[3] Mourou G A *et al* 2006 Optics in the relativistic regime *Rev. Mod. Phys.* **78** 309–70

[4] Lontano M and Passoni M 2007 *Progress in Ultrafast Intense Laser Science (Springer's Review Book Series* Vol II) (Berlin: Springer) chapter 17

[5] Wilks S C *et al* 2001 Energetic proton generation in ultra-intense laser–solid interactions *Phys. Plasmas* **8** 542

[6] Macchi A *et al* 2005 Laser acceleration of ion bunches at the front surface of overdense plasmas *Phys. Rev. Lett.* **94** 165003

[7] Robinson A P L *et al* 2008 Radiation pressure acceleration of thin foils with circularly polarized laser pulses *New J. Phys.* **10** 013021

[8] Robinson A P L *et al* 2009 Relativistically correct hole-boring and ion acceleration by circularly polarized laser pulses *Plasma Phys. Control. Fusion* **51** 024004

[9] Ceccotti T *et al* 2007 Proton acceleration with high-intensity ultrahigh-contrast laser pulses *Phys. Rev. Lett.* **99** 185002

[10] Passoni M *et al* 2004 Charge separation effects in solid targets and ion acceleration with a two-temperature electron distribution *Phys. Rev. E* **69** 026411

[11] Mora P 2003 Plasma expansion into a vacuum *Phys. Rev. Lett.* **90** 185002

[12] Bychenkov Yu V *et al* 2004 Ion acceleration in expanding multispecies plasmas *Phys. Plasmas* **11** 3242

[13] Mora P 2005 Thin-foil expansion into a vacuum *Phys. Rev. E* **72** 056401

[14] Betti S *et al* 2005 Expansion of a finite-size plasma in vacuum *Plasma Phys. Control. Fusion* **47** 521

[15] Tikhonchuk V T *et al* 2005 *Plasma Phys. Control. Fusion* **47** B869

[16] Brantov A V *et al* 2009 Laser-triggered ion acceleration from a double-layer foil *Phys. Plasmas* **16** 043107

[17] Albright B J *et al* 2006 Theory of laser acceleration of light-ion beams from interaction of ultrahigh-intensity lasers with layered targets *Phys. Rev. Lett.* **89** 115002

[18] Nishiuchi M *et al* 2006 The laser proton acceleration in the strong charge separation regime *Phys. Lett.* A **357** 339–44

[19] Passoni M *et al* 2004 One-dimensional model of the electrostatic ion acceleration in the ultraintense laser–solid interaction *Laser Part. Beams* **22** 163

[20] Lontano M *et al* 2006 Electrostatic field distribution at the sharp interface between high density matter and vacuum *Phys. Plasmas* **13** 042102

[21] Passoni M *et al* 2008 Theory of light-ion acceleration driven by a strong charge separation *Phys. Rev. Lett.* **101** 115001

[22] Kar S *et al* 2008 Dynamic control of laser-produced proton beams *Phys. Rev. Lett.* **100** 105004

[23] Quinn K *et al* 2009 Laser-driven ultrafast field propagation on solid surfaces *Phys. Rev. Lett.* **102** 194801

[24] Cercignani C and Kremer G M 2002 *The Relativistic Boltzmann Equation: Theory and Application* (Basel: Birkhäuser)

[25] Wilks S C *et al* 1992 Absorbtion of ultra-intense laser pulses *Phys. Rev. Lett.* **69** 1383

[26] Gibbon P 2005 *Short Pulse Laser Interactions with Matter: An Introduction* (London: Imperial College Press)

[27] McKenna P *et al* 2004 Characterization of proton and heavier ion acceleration in ultrahigh-intensity laser interactions with heated target foils *Phys. Rev.* E **70** 036405

[28] Mackinnon A J *et al* 2002 Enhancement of proton acceleration by hot-electron recirculation in thin foils irradiated by ultraintense laser pulses *Phys. Rev. Lett.* **88** 21

[29] Fritzler S *et al* 2003 Proton beams generated with high-intensity lasers: applications to medical isotope production *Appl. Phys. Lett.* **83** 15

[30] Kaluza M *et al* 2004 Influence of the laser prepulse on proton acceleration in thin-foil experiments *Phys. Rev. Lett.* **93** 4

[31] Fujii T *et al* 2003 MeV-order proton and carbon ion acceleration by irradiation of 60 fs TW laser pulses on thin copper tape *Appl. Phys. Lett.* **83** 8

[32] Spencer I *et al* 2003 Experimental study of proton emission from 60-fs, 200-mJ high-repetition-rate tabletop-laser pulses interacting with solid targets *Phys. Rev.* E **67** 046402

[33] Nishiuchi M *et al* 2008 Efficient production of a collimated MeV proton beam from a polyimide target driven by an intense femtosecond laser pulse *Phys. Plasmas* **15** 053104

[34] Borghesi M *et al* 2009 Laser-driven proton acceleration and applications: recent results *Eur. Phys. J. Spec. Top.* **175** 105–10

[35] Fuchs J *et al* 2009 Laser acceleration of low emittance, high energy ions and applications *C. R. Phys.* **10**

[36] Oishi Y *et al* 2005 Dependence on laser intensity and pulse duration in proton acceleration by irradiation of ultrashort laser pulses on a Cu foil target *Phys. Plasmas* **12** 073102

[37] Zepf M *et al* 2001 Fast particle generation and energy transport in laser–solid interactions *Phys. Plasmas* **8** 5

[38] Roth M *et al* 2002 Energetic ions generated by laser pulses: a detailed study on target properties *Phys. Rev. Spec. Top. Accel. Beams* **5** 061301

[39] Borghesi M *et al* 2006 Fast ion generation by high-intensity laser irradiation of solid targets and applications *Fusion Sci. Technol.* **49** 412

[40] Borghesi M *et al* 2008 Laser driven proton acceleration: source optimization and radiographic applications *Plasma Phys. Control. Fusion* **50** 124040

[41] Passoni M *et al* 2009 Proton maximum energy cutoff scaling laws for bulk targets *AIP Conf. Proc.* **1153** 159

[42] Passoni M *et al* 2010 Target normal sheath acceleration at ultrahigh intensities: a theoretical parametric investigation *AIP Conf. Proc.* submitted

[43] Passoni M *et al* 2010 Energetic ions from next generation ultraintense ultrashort lasers: scaling laws for target normal sheath acceleration *Nucl. Instrum. Methods Phys.* A at press

[44] Esirkepov T *et al* 2006 Laser ion-acceleration scaling laws seen in multiparametric particle-in-cell simulations *Phys. Rev. Lett.* **96** 105001